Plasma Monitoring of Laser Beam Welds

Light and sound intensity measurements can be used for the monitoring of plasma initiation and propagation during laser beam welding

BY G. K. LEWIS AND R. D. DIXON

ABSTRACT. Experimental and theoretical studies using high power density laser pulses (greater than 10^9 W/cm^2) at pulse lengths less than 1 microsecond have proven the existence of laser supported absorption waves. In our ND:YAG laser beam welding power and pulse regimes (400 watts maximum average power with pulse durations of 0.5-8 ms), high speed photography, microphone, and light intensity measurements show that multiple laser supported waves form during a single pulse and produce enhanced coupling with the target.

Introduction

The use of lasers for welding and materials processing has become an important manufacturing process. The Nd:YAG (1.06 μm)* and CO_2 (10.6 μm)* lasers have evolved into primary tools for laser beam welding operations. Typical Nd:YAG systems are pulsed with average powers up to 400 watts, while CO_2 systems may be pulsed or continuous wave with average powers up to 20 kilowatts. These systems are used on a wide range of metals for low heat input, high precision welds.

At the Los Alamos National Laboratory, a significant effort is in progress to develop techniques for controlling and certifying the laser beam welding process. Initial weld morphology vs. weld variable studies indicated a large variation in depth of joint penetration for any one set of laser conditions, particularly on high reflectivity materials. The data, along with the appreciation that more must be known about the process, led to experiments using acoustic emission as a monitoring technique. These studies showed significant acoustic energy generation but no apparent correlation with weld morphology. The affect of the plasma was not considered in these studies. As a result, a literature review and experimental study were performed to determine the laser light-plasma-material interaction process and the affect on welding.

Theoretical and experimental studies, primarily at power densities much greater than 10^9 W/cm^2 and pulse lengths of less than 1 microsecond (μs) duration, have attempted to characterize the laser-plasma-target interaction (Refs. 1-25). These studies have shown that the interaction involves many variables such as the type of plasma formed, laser light intensity, wavelength, interaction time, energy spatial and temporal distribution, environment above the target, surface conditions, target composition, and material physical properties, among others. Although far removed from the laser beam welding power regime of $10^4 - 10^9$ W/cm^2 and pulse durations of several milliseconds to continuous wave, these studies have provided information applicable to the plasma effects occurring during laser beam welding.

This paper deals with the laser-plasma-material interaction as experienced with a Raytheon Nd:YAG laser in the pulsed mode at average power levels up to 400 watts. In this power regime, we are concerned primarily with low joint penetration welds on the order of 1.5-3.0 mm (0.06-0.12 in.) penetration. The results of our studies are applicable to this welding regime, and we have not extended the same experimental tests to the multikilowatt deep joint penetration welds made with industrial CO_2 lasers.

Although the same plasma theory explained in the text applies to the higher multikilowatt power levels, the CO_2 lasers produce different plasma waves with different characteristics than the LSC waves experienced in the lower power regime of the Nd:YAG. The type of plasma wave produced depends on the power density of the laser beam. Hence, the laser-plasma interaction may change as power is increased. Other effects such as radiation trapping during deep joint penetration keyhole welding are not significant at the power levels discussed here.

Laser-Plasma-Material Interaction

Absorption of laser energy depends initially on the intrinsic absorptivity of the target material. Absorptivity generally increases with decreasing wavelength; it may increase because of a change in metal temperature, base metal oxidation state or other surface reaction.

Figure 1 shows the spectral reflectance (reflectance equals 1-absorptivity) for various elements at room temperature. At the Nd:YAG and CO_2 wavelengths (1.06 and 10.6 μm, respectively), less than 10% of the light is absorbed by Al and less than 5% by Cu, Ag and Au. Absorption of the laser radiation typically does not account for the amount of material melted during the welding process, particularly for highly reflective materials. Instead, an increase in coupling efficiency is noted as laser intensities are increased above plasma initiation threshold intensities. This phenomenon is referred to as "enhanced coupling" (Ref. 18) and is related to the plasma formation and subsequent radiation heating of the base metal by the plasma.

The significance of the radiant heat flux from the plasma to the base metal is shown in Fig. 2 and equation (1). As the

*1μm (micrometer) = 0.00004 in.

Based on a paper sponsored by the DOE Interagency Group for presentation at the 64th Annual AWS Convention held in Philadelphia, Pennsylvania, during April 24-29, 1983.

G. K. LEWIS and R. D. DIXON are with the Materials Science and Technology Division, Los Alamos National Laboratory, Los Alamos, New Mexico.

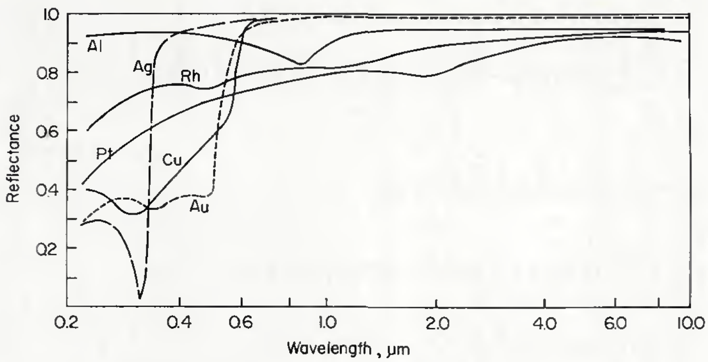

Fig. 1—Reflectance as a function of wavelength

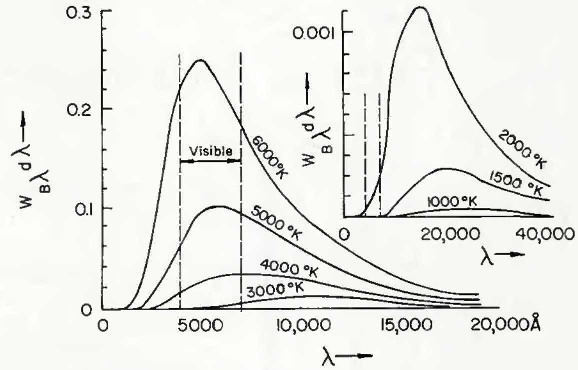

Fig. 2—Blackbody energy flux emitted as a function of wavelength and temperature

temperature of the plasma increases, the maximum energy flux emitted increases by the fourth power of temperature and shifts towards shorter wavelengths. The short wavelengths are more readily absorbed than the infrared laser radiation as shown in Fig. 1. The total energy emitted, assuming the plasma radiates as a black body, is given by the Stefan-Boltzmann law:

$$W_\beta = \sigma \Upsilon^4 \quad (1)$$

where $\sigma = 5669 \times 10^{-5}$ erg cm^{-2} s^{-1} k^{-4} and Υ = absolute temperature.

Laser plasmas typically reach temperatures of 5000-20,000 K (Ref. 1) and thus can contribute a significant amount of heat to the part. However, calculation of the heat flux from plasma to target must account for changing plasma temperature due to plasma density, velocity, volume and other factors that are difficult to measure. An upper limit of such a calculation assumes that the laser light is totally absorbed by the plasma and yields an absorption of energy by the material of 50% of the incident laser energy (Ref. 1). This is a significant improvement over the 1-10% absorbed without the plasma.

Because the plasma formation significantly affects the welding process, initiation and propagation mechanisms must be understood. Incident laser light partially absorbed by the target and surrounding medium causes heating, vaporization of asperites at high energy density sites, electron emission and ion emission (Ref. 20-25). The electron, ion, and neutral atoms constitute a plasma that ignites and absorbs the incident laser energy when the plasma temperature and density become high enough. Additional mechanisms contribute to the plasma formation for low power laser systems. The most dominant are: thermoelectron emission, photo-electron emission and inverse "bremstrallung" in the medium above the target.

The ignition is signalled by the creation of a laser supported absorption (LSA) wave and is preceded by a pressure pulse that propagates away from the target leaving a shocked region for the absorption wave to propagate into. This process is shown schematically in Fig. 3 (from Ref. 1) with the regions for the relevant plasma variables: pressure (P), density (ρ), particle velocity (U), temperature (Υ), enthalpy (h) with spatial coordinates X and L. The subscript S refers to the shock region and the subscript ∞ refers to ambient conditions. Note the laser is incident from the left and that the absorption wave has been identified as a Laser Supported Combustion (LSC) wave with velocity (v_w).

Laser-target interactions produce two distinct types of absorption waves: the previously mentioned LSC wave and a laser supported detonation (LSD) wave. Both waves contribute to enhanced coupling, but the LSC wave is optimal. Pirri, Kemp, Root and Wu (Ref. 1), among other investigators, have modeled the plasma wave formations and characteristics. Some of their results are discussed below, and their models are shown in Figs. 3-5.

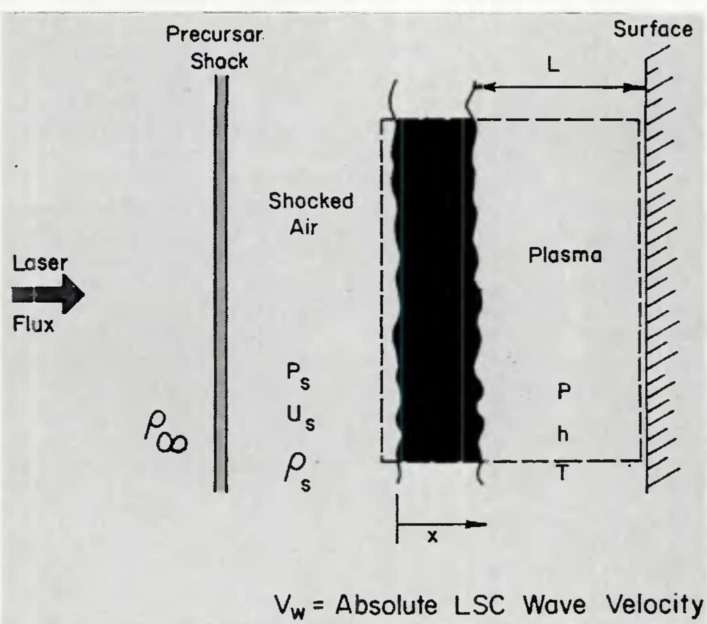

Fig. 3—Schematic representation of a LSC wave (Ref. 1)

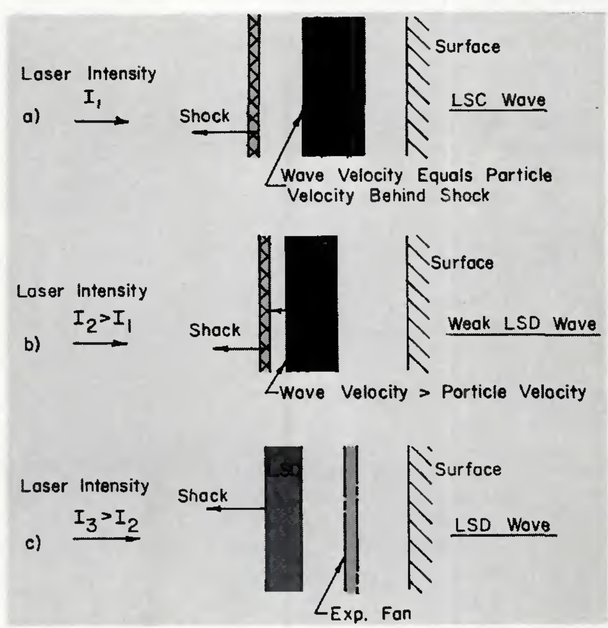

Fig. 4—Transition from LSC to LSD wave (Ref. 1)

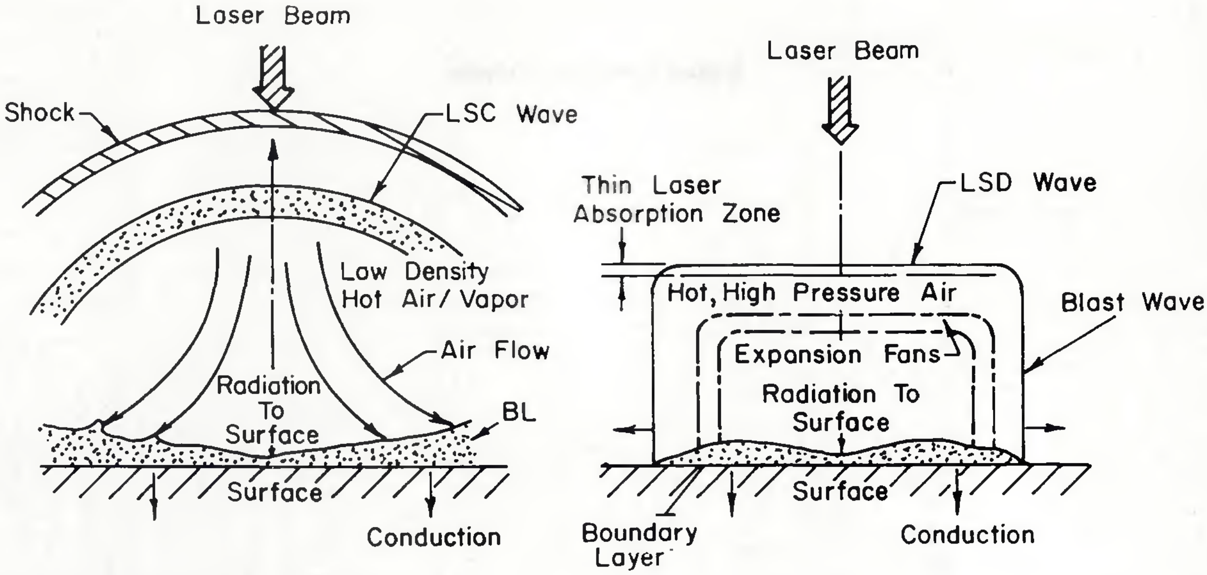

Fig. 5 — Two-dimensional LSC and LSD waves (Ref. 1)

After plasma initiation the absorption wave will propagate into shocked space. The absorption wave velocity and the conditions within the shocked space behind the precursor determine the type of absorption wave. If the precursor wave imparts sufficient energy to the air (environment) to cause absorption of the incident laser energy, then the absorption wave created travels at the shock wave velocity causing considerable mass flow through the wave. Such a wave is denoted as a LSD wave.

If the shock is not energetic enough to allow the shocked gas to absorb the laser energy, then the absorption wave follows the shock wave at a lower velocity and the driving energy is from the plasma radiation produced by absorption of laser light in the plasma. This wave is known as a LSC wave and is characterized with subsonic wave velocity and less mass transport compared to the LSD wave. Because the plasma temperature depends upon the input energy rate and the mass flow rate, the LSD wave will contribute less radiant heat to the base metal than the LSC wave.

The conditions for transition from a combustion to detonation wave are shown in Fig. 4. Figure 4A represents a LSC wave propagating into shocked gas at a velocity less than or equal to the shocked gas particle velocity. As the laser intensity is increased, an absorption wave is created that has a velocity greater than the shocked particle velocity. Such a wave is not quite a LSC or LSD wave and is denoted as a weak LSD wave as shown in Fig. 4B. When the laser intensity is very high, the shocked region absorbs the laser energy and a LSD wave is generated; the latter condition is shown in Fig. 4C. Figure 5 gives a two-dimensional representation of the LSC and LSD waves; it shows some of the more salient features such as the surface boundary region and the blast wave within expansion fans seen in the LSD waves.

Calculations from one dimensional LSC wave theory (Ref. 1) show that, after ignition by a 1×10^5 watt-cm^{-2} CO_2 laser, a LSC wave will travel 2 cm (0.79 in.) in less than 100 μs. Two dimensional calculations (Ref. 16) for 1×10^6 watt-cm^{-2} CO_2 laser radiation show that a high temperature isotherm closes upon itself in the 2–3 cm (0.79–1.18 in.) region in less than 100 μs, suggesting separation of the plasma wave from the target surface. Most laser welding occurs at times greater than 100 μs; this implies that a series of LSC waves will continually initiate, propagate and decay during the welding pulse.

Experimental Description

The models for LSA waves suggest several diagnostics to correlate the plasma initiation, growth and regeneration to the laser pulse and resultant target affects. Each LSA wave formation is characterized by a precursor shock wave followed by a visible plasma wave that propagates away from the target. The plasma process can be monitored by using a microphone to detect the shock wave and a photomultiplier to detect visible light from the plasma. The signals are correlated to the laser pulse characteristics and high speed photography shown schematically in Fig. 6.

A pulsed Nd:YAG (1.06 micron wavelength) laser (Raytheon Model SS500) capable of a maximum average power of 400 watts was used for this study. The pulse length could be varied from 0.5–8.0 ms. Single pulse welds were made at visual sharp focus on base metal surfaces without an aperture in the beam path. The power was measured for each power condition using a Coherent Model 213 power meter. The laser pulse shape was temporarily monitored on an oscilloscope using a detector on the back of the laser cavity coupled with a 0.01% transmitting rear cavity mirror.

Plasma shock waves were monitored by a Buehl and Kjaer microphone with a 200 Hz to 20 kHz range. The microphone was placed approximately 12.5 mm (approx. ½ in.) from the focal spot. Visible plasma light was monitored with a photomultiplier tube (PMT) having a S-20 response. The tube was coupled to the laser spot by a fiber optic light guide placed within 12.5 mm (0.49 in.) of the focal spot of the laser beam. The fiber had a 30 deg included angle cone of acceptance. The PMT was not sensitive to 1.06 μm light from the laser.

High speed movies were taken at 4000 frames per second with black and white negative film. A light inside the film cavity turned on with the event trigger pulse and exposed one edge of the film for a starting time reference. Timing marks were placed on the film for speed calculations.

A four channel digital oscilloscope was used to record the diagnostic signals at a rate of 5 μs/point. The scope was triggered by a logic circuit that output a trigger pulse when the laser shutter was open and the next laser pulse occurred. The trigger pulse started the sweep on the scope and turned the light on inside the movie camera.

All targets were 2.22 cm (0.874 in.) diameter by 0.15 cm (0.059 in.) thick discs. The discs were mounted on a rotary base to index the target on a common axis. The target materials were Type 304 stainless steel, 5052 aluminum

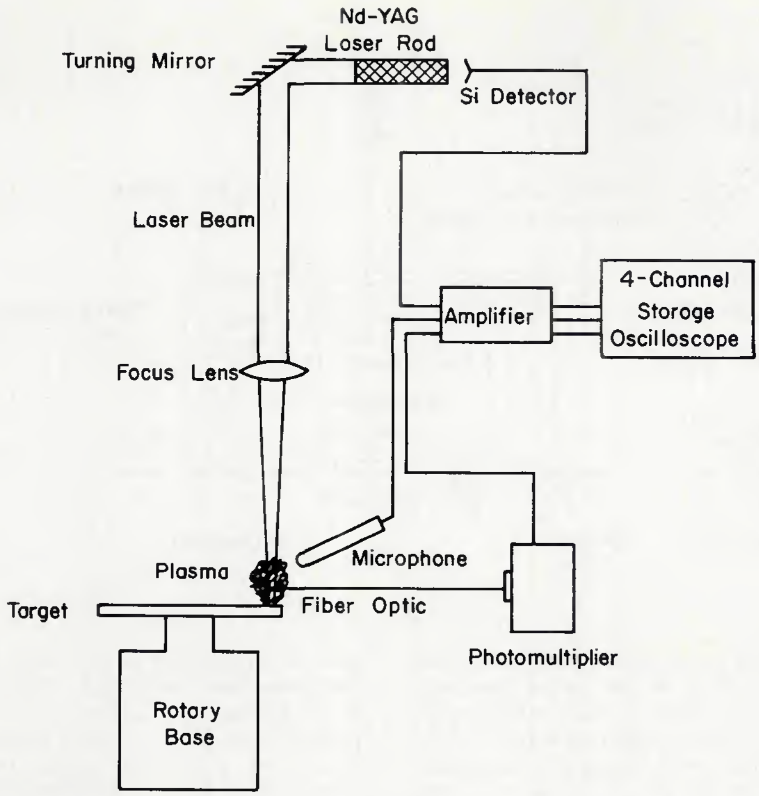

Fig. 6 — Laser plasma diagnostics experimental set up

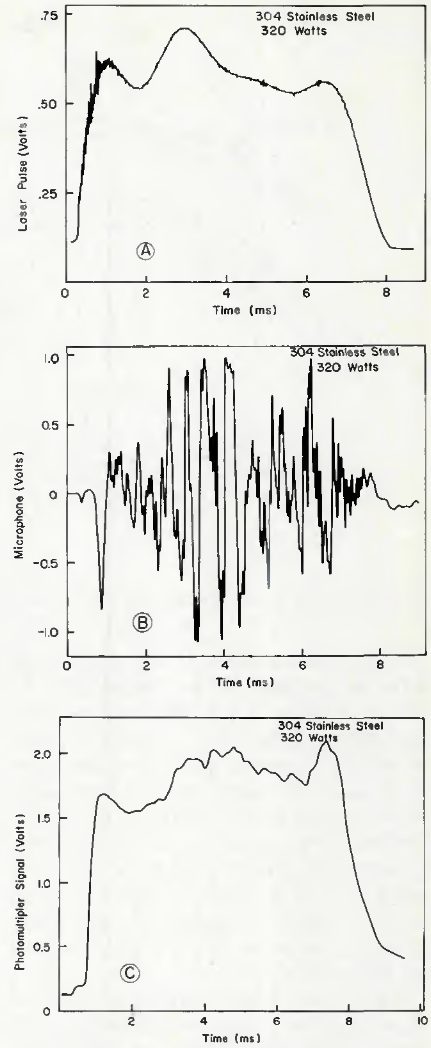

Fig. 7 — Signals for Type 304 stainless steel at 320 W average power and 8 ms pulse: A — laser; B — microphone; C — photomultiplier

alloy, and pure gold. These materials were chosen to be representative of both high reflectivity and low reflectivity materials. Single spot welds were made on each material at 320 watts and 70 watts average power at a pulse length of 8.0 ms. Each target was swabbed with alcohol just prior to making the spot weld.

Results and Discussion

Typical signals recorded for 320 watts average power laser pulses on Type 304 stainless steel, 5052 aluminum alloy and coated gold are shown in Figs. 7–9. The relative signal intensities are not significant, because the gains and detector distances from the source were varied depending on material. It was observed that the signals recorded from the Type 304 stainless steel plasmas were of much greater intensity than the signals from the 5052 aluminum alloy and pure gold plasmas.

The most prominent features of these signals are the multiple peaks shown in the microphone and photomultiplier curves. These peaks indicate that many plasma waves form sequentially during a single 8 ms laser pulse. Each major microphone peak and associated ring down represents a precursor shock wave, and each slope change and inflection point in the photomultiplier signal represent plasma initiation and propagation past the fiber optic detector.

The microphone and photomultiplier signals were correlated in time by comparing peak times for both signals. These times correlated well in many cases, particularly in the beginning stages of plasma initiation. In each microphone signal shown, an intense negative spike indicates the start of multiple plasma regeneration and may be correlated to peaks or slope changes that are slightly later in time on the photomultiplier signals. These correlations are masked somewhat by microphone ringdown and by the integration of the plasma wave light intensity signals caused by the wide cone of acceptance of the fiber optic detector.

Photographs of the plasma formations for the data in Fig. 7 are shown in Fig. 10. Each frame represents an integrated event time of 250 μs. The first small negative microphone signal was at t = 0.38 ms corresponding to the first visible plasma formation in the frame representing t = 0.25 ms to t = 0.50 ms. The photomultiplier data in Fig. 7B show the first rise in signal intensity initiating at 0.38 ms and continuing to rise until t = 0.57 ms where the intensity levels off. The large negative peak in the microphone signal starts at t = 0.73 ms and continues to t = 0.90 ms corresponding to the steep increase in the photomultiplier tube signal starting at t = 0.73 ms and ending at t = 1.0-1.25 ms where the plasma propagates out of the picture.

Similar correlations may be made for the photographs in Figs. 11 and 12 with the data in Figs. 8 and 9, respectively, for 5052 aluminum alloy and coated gold. The photographs shown correspond to signal changes for the first parts of the laser pulse. At times greater than those shown in Figs. 10–12, many plasmas were formed and propagated higher than the height of the picture until the laser pulse ended.

In comparing the plasma data for the three materials studied, the Type 304 stainless steel plasmas initiated earlier during the laser pulse and regenerated other plasmas more rapidly than in the tests on 5052 aluminum alloy and coated gold. In tests at 70 watts average power, plasmas were initiated to a lesser extent for Type 304 stainless steel and 5052 aluminum alloy and not at all for pure gold without a coating. For pure gold without a coating

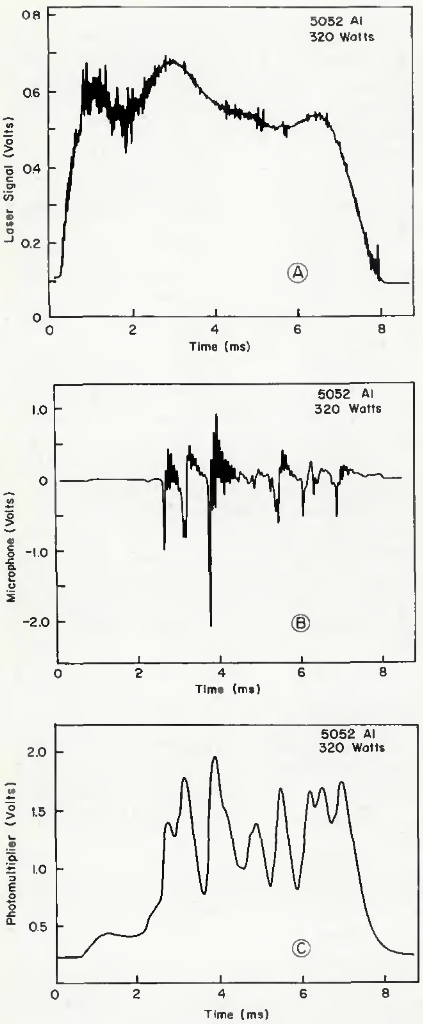

Fig. 8—Signals for 5052 aluminum alloy at 320 W average power and 8 ms pulse: A—laser; B—microphone; C—photomultiplier

at 320 watts, a very small plasma was barely visible on the 4000 fps film. The addition of an ink coating using the same laser parameters produced multiple plasmas during the pure gold test. In each case where plasma formation and regeneration were not detected, there was no visible melting of material. As the number of LSA waves increased, either by increasing laser power or by application of a coating in the case of Au, the amount

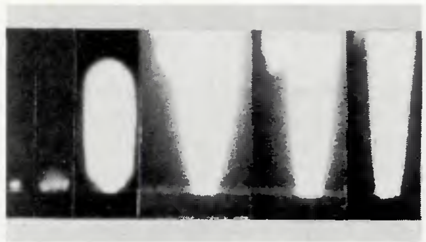

Fig. 10—Photographs at 4000 fps corresponding to data in Fig. 7. From left to right, pictures represent 0.25 ms intervals starting at event time = 0.25 ms. ×5.6 (reduced 40% on reproduction)

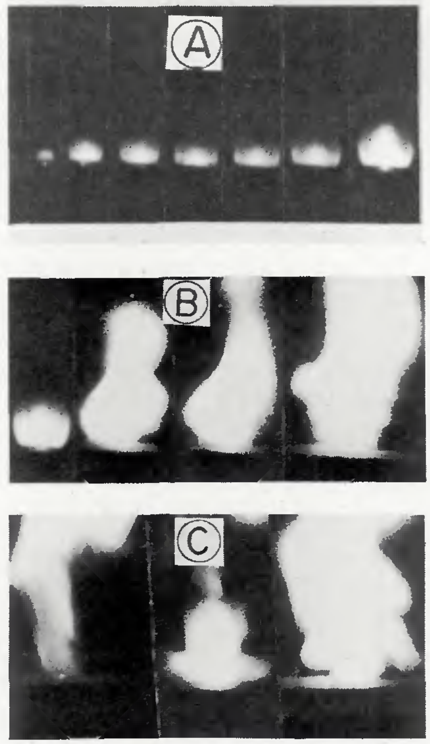

Fig. 11—Photographs at 4000 fps corresponding to data in Fig. 8. From left to right, pictures represent 0.25 ms intervals starting at event times as follows: A—0.45 ms; B—2.45 ms; C—3.45 ms. ×5.6. With reductions as follows on reproduction: A—28%; B—38%, C—40%

of molten material increased.

The change in the number of plasmas formed with power increase or surface modification suggests that a plasma initia-

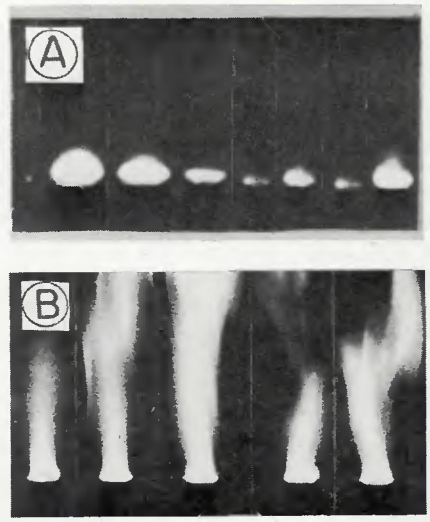

Fig. 12—Photographs at 4000 fps corresponding to data in Fig. 9. From left to right, pictures represent 0.25 ms intervals starting at event times as follows: A—0.60 ms; B—2.60 ms. ×5.6 with reductions as follows on reproduction: A—27%; B—50%

tion energy threshold must be crossed to start the plasma regeneration process. Once that energy level is exceeded, a LSA wave is formed and propagates up the beam. The LSA wave allows some fraction of the incident laser fluence to reach the target. If that amount of energy plus the plasma radiant energy is less than the plasma initiation threshold, a second plasma cannot form. As the wave propagates up the focused beam, it may decrease in density because of increased turbulence or lower laser power density and allow a larger fraction of incident laser light to reach the target. At some time during the life of the wave, the fraction of incident light allowed through will exceed the plasma threshold energy, and another LSA wave can form and propagate away from the surface.

Conclusion

Plasma initiation and propagation during laser welding can be monitored by measuring the light intensity and sound intensity that is characteristic of a laser supported absorption wave. The number

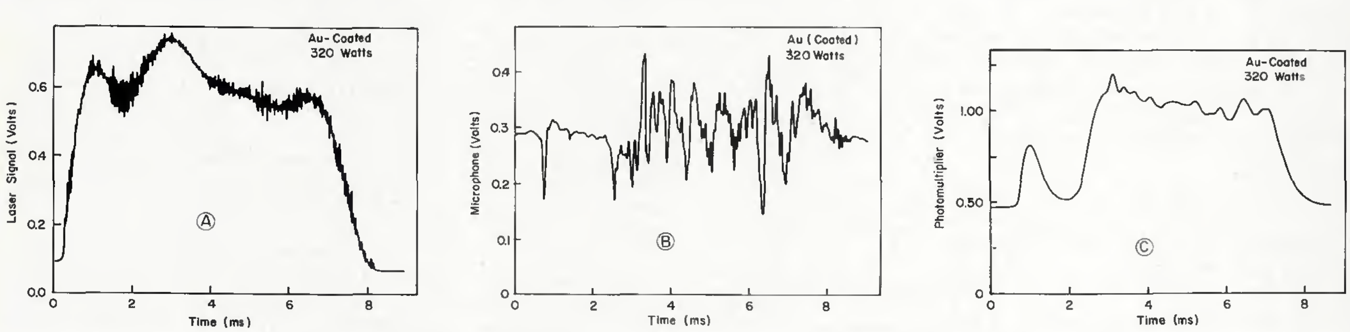

Fig. 9—Signals for gold (coated) at 320 W and 8 ms pulse: A—laser; B—microphone; C—photomultiplier

RESEARCH/DEVELOPMENT/RESEARCH/DEVELOPMENT/RESEARCH/DEVELOPMENT/RESEARCH/DEVELOPMENT

of plasmas produced during a single 8 ms laser pulse depends on substrate material, surface condition and laser power density. The amount of melting increases as the number of plasma regenerations increases; this suggests that radiant heating from the plasma is an important heating mechanism during the laser beam welding process. An ink coating used on a gold target increased the number of plasmas formed and increased the amount of molten material formed compared to gold without a coating.

Process Monitoring of Laser Beam Welds

The experiments described have attempted to characterize the interaction between the incident laser light, the plasma formation and the target material during pulse welding with a Nd:YAG laser. Although the overall laser beam welding process is complex, the instruments used in these tests may lead to a method of real time monitoring, at least in our Nd:YAG welding regime of average powers up to 400 watts.

At present, microphones and fiber optic light detectors are used to signal plasma initiations and propagation. The number of plasmas generated appears to correlate with the weld pool penetration in a target. Velocities of plasma shock waves moving away from the target can be calculated by spacing the microphones at a known distance and measuring the time interval between microphone signals for any single plasma initiation. The wave velocity characterizes the wave as LSC (subsonic) or LSD (supersonic). The presence of LSC waves indicates that enhanced coupling may dominate the process, implying that radiation from the plasma is contributing significantly to the weld pool depth.

Ideally, plasma temperature data coupled with the velocity and initiation data would allow calculation of the radiation flow to the target. Temperature measurement can be made by measuring plasma density with time but is complex. However, comparison of numbers of plasmas and their velocities with depths of penetration at various laser settings can be made and a relative evaluation of penetration depth established. If the wave is LSD, other factors such as reflection of laser light from the plasma may become significant and decrease the enhanced coupling affect. The LSD wave regime is recommended as the subject of future work.

The instrumentation described for such a monitor is practical from the standpoint of size and non-interference with the welding process. Microphones 8–12 mm (0.31–0.47 in.) diameter and fiber optic strands 0.2–1.0 mm (0.008-0.04 in.) can easily be attached to the laser focusing head to follow the weldment. Plasma activity could be monitored with statistical sampling at various points along the weldment for analysis.

The monitoring technique described is by no means complete. However, it would help in identifying the power regimes where the phenomenon of enhanced coupling is significantly changing the amount of energy coupled to the target surface. An improved monitor must account for the energy balance for the entire process. Such a monitor requires spatial and temporal characterization of the laser pulse, measurement of the absorbed and reflected light at the material surface and measurement of the absorbed, transmitted and reflected light from the plasma. Work in these areas is continuing to understand the laser beam welding process more completely than is presently known and to develop the monitoring instrumentation required.

Acknowledgments

The authors wish to acknowledge the assistance and expertise of the following people: Mike Ward, EG&G, Los Alamos—set up the instrumentation and fiber optics for the plasma light intensity measurements; Tony Rollett and John Buchen, Los Alamos National Laboratory—wrote the data reduction computer program and designed the triggering circuit for data acquisition, respectively; Carolina Munoz, University of Texas, El Paso—correlated diagnostic signals to high speed photographs. In memoriam, Robb Gordon, Los Alamos National Laboratory—photographed the plasma formations at 4000 fps.

References

1. Pirri, A. N., Kemp, N. H., Root, R. G., and Wu, R. K. S. 1977 (Jan.). *Theoretical laser effects studies.* Final report, PSI-TR-89. Physical Sciences, Inc.

2. Boni, A. A., Su, F. V., Thomas, P. D., and Musal, H. M. 1977 (April). *Theoretical study of laser target fabrication.* Final report, SAI-77-567 LJ. Science Applications, Inc.

3. Casey, H. 1980 (Sept.). *Plasma phenomena during Nd-YAG laser welding.* Sixth International Conference of the Institute of Electrical Engineers/Welding Institute, Edinburgh, UK.

4. Nichols, D. B., and Hall, R. B. 1978. Threshold conditions for the formation of surface plasmas by HF and DF laser radiation. *J. Applied Physics.* 49(10):5155-5169.

5. Godwin, R. P. 1979. Absorption in laser-produced plasma experiments: a personal view. *Applied Optics* 18(21):3555-3561.

6. Jaonimagi, P. A., and Richardson, M. C. 1983. Time resolved x-ray photography of the expansion of nanosecond CO_2 laser produced plasmas. *Optics Communications* 44(3):180-184.

7. Maher, W. E., Hall, R. B., and Johnson, R. R. 1974. Experimental study of ingnition and propagation of laser-supported detonation waves. *Journal of Applied Physics* 45(5):2138-2145.

8. McKay, J. A., Bleach, R. D., Nagel, D. J., and Schriemph, J. T. 1979. Pulsed-CO_2-laser interaction with aluminum in air: thermal response and characteristics. *Journal of Applied Physics* 50(5):3231-3240.

9. Walters, C. T., Barnes, R. H., and Beverly, R. E. 1978. Initiation of laser-supported-detonation (LSD) waves. *Journal of Applied Physics* 49(5):2937-2949.

10. Krokhin, O. N. 1972. Generation of high-temperature vapors and plasmas by laser radiation. *Laser handbook,* eds. F. T. Arecchi and E. O. Schulz-DuBois, pp. 1371-1406. North-Holland Publishing Co.

11. Pirri, A. N., Root, R. G., and Wu, P. K. S. 1978. Plasma energy transfer to metal surfaces irradiated by pulsed lasers. *AIAA Journal* 15(12):1296-1304.

12. McKay, J. A., and Schriempf, J. T. 1979. Transient surface heating of metals by CO_2 laser pulses with air-plasma ignition. *Journal of Applied Physics* 50(8):5202-5205.

13. Beverly, R. E., and Walters, C. T. 1976. Measurements of CO_2-laser-induced shocked pressures above and below LSD-wave thresholds. *Journal of Applied Physics* 47(8):3485-3495.

14. Raizer, Q. P. 1965. Heating of a gas by a powerful light pulse. *Soviet Physics JEPT* 21(5):1009-1017.

15. Basov, N. G., Gribkov, V. A., Korkhin, O. N., and Sklizkov, G. V. 1968. High temperature effects of intense laser emission focused on a solid target. *Soviet Physics JEPT* 27(4):575-582.

16. Jackson, J. P., and Nielsen, P. E. 1974. Ignition transients and two-dimensional effects in the propagation of laser-supported-absorption waves. *Laser Digest,* report AFWL-TR-74-100:212-226.

17. Boni, A. A., and Su, F. Y. 1974. Propagation of laser supported deflagration waves. *The Physics of Fluids* 17(2):340-342.

18. Marcus, S., Lowder, J. E., and Mooney, D. L. 1976. Large spot thermal coupling of CO_2 laser radiation to metallic surfaces. *Journal of Applied Physics* 17(7):2966-2968.

19. Dimitrijevic, M., and Konjevic, N. 1980 (June). The importance of the pulse shape for the laser-beam target interaction. *Optics and laser technology,* pp. 145-147.

20. Smith, D. C. 1971. Gas breakdown dependence on beam size and pulse duration with 10.6 μm wavelength radiation. *Applied Physics Letters* 19(10):405-408.

21. Smith, D. C. 1979 (Aug.). Laser induced gas breakdown and plasma shielding. *SPIE* 195:171-181.

22. Smith, D. C., and Brown, R. T. 1975. Aerosol-induced air breakdown With CO_2 laser radiation. *Journal of Applied Physics* 46 (3):1146-1154.

23. Smith, D. C., and Fowler, M. C. 1973. Ignition and maintenance of a CW plasma in atmospheric-pressure air with CO_2 laser radiation. *Applied Physics Letters* 22(10):500-502.

24. Smith, D. C. 1977. Gas breakdown initiated by laser radiation interaction with aerosols and solid surfaces. *Journal of Applied Physics* 48(6):2217-2225.

25. Fowler, M. C., and Smith, D. C. 1975. Ignition and maintenance of subsonic plasma waves in atmospheric pressure air by CW CO_2 laser radiation and their effect on laser beam propagation. *Journal of Applied Physics* 46(1):138-149.